Physical Modeling of PM Synchronous Motors for Integrated Coupling With Machine Drives

O. A. Mohammed, *Fellow, IEEE*, S. Liu, *Senior Member, IEEE*, and Z. Liu

Department of Electrical and Computer Engineering, Energy Systems Laboratory, Florida International University, Miami, FL 33174 USA

A physical phase variable model for permanent magnet synchronous motors is proposed. This model is initiated to pursue an accurate and fast motor model for integrated motor drive simulation. Since the full finite element (FE) model may be time consuming and the direct- and quadratic-axis (dq)-model is inaccurate, the proposed physical phase variable model eliminates these deficiencies. The proposed model is a circuit model with inductance, back electromotive force (EMF), and cogging torque calculated from nonliner transient FE solutions. The main characteristics of this model are that it is as accurate as the full FE model while giving fast computational results. The Simulink implementation of the proposed model is studied. Comparisons of the proposed model with the full FE model and the dq-model are performed. The results verify the validity of the proposed model and show its practical superiority in drives applications.

***Index Terms*—Finite element analysus (FEA), integrated motor drive, PM synchronous motor, phase variable model.**

I. Introduction

THE direct- and quadratic-axis (dq)-model is established based on the assumption that both the working flux distribution and the winding flux linkage are sinusoidal. There are two types of effects which are ignored by the dq-model. One relates to the geometrical structure, for example, the effects of slotting, the shape of the rotor iron, magnet surface, etc. The other relates to the nonlinear magnetization property of iron core material including the effects of saturation, unequal mutual inductances due to asymmetric magnetization, etc. The ignored effects bring the inaccuracy to the dq-model.

The finite element (FE) model takes into consideration all these effects ignored by the dq-model. As a result, the working flux at the air gap and the winding flux linkage includes harmonic components. Compared with the dq-model, the FE model gives accurate results but it is time consuming.

A physical phase variable model is proposed in this paper. It is a circuit model, whose parameters are obtained from the nonliner transient FE solutions of the machine. It provides fast simulation speed with the same performance level as the results obtained using the full FE model. A permanent magnet (PM) surface mounted synchronous motor in a drive system is used as an example. The equations of the physical phase variable model, its parameter acquisition, as well as its Simulink implementation are presented. Comparisons of the proposed model with dq-model and the full FE model are performed.

II. Physical Phase Variable Model

The proposed physical phase variable model for PM synchronous machines is given below. The voltage, torque, and the motion equations are [1]–[3]

$$V_{abc} = r_{abc} i_{abc} + \frac{d\psi_{abc}(i_{abc},\theta)}{dt} \tag{1}$$

$$\psi_{abc}(i_{abc},\theta) = L_{abc}(\theta) i_{abc} + \psi_{rabc}(\theta) \tag{2}$$

$$T_m = p\left(\frac{1}{2} i_{abc}^T \cdot \frac{dL_{abc}(\theta)}{d\theta} \cdot i_{abc} + i_{abc}^T \cdot \frac{d\psi_{rabc}(\theta)}{d\theta}\right) + T_{\text{cog}}(\theta) \tag{3}$$

$$J \cdot \frac{d\omega}{dt} = T_m - B\omega - T_L \quad \text{and} \quad \frac{d\theta}{dt} = \omega \tag{4}$$

where V_{abc}, i_{abc}, and r_{abc} are the terminal voltage, phase current, and winding resistance. T_m and T_L are the output torque and the load torque. p, J, and B are the number of pole pairs, inertia, and friction factor. ω is the angular speed.

θ is the rotation angle/rotor position. $T_{\text{cog}}(\theta)$ is the cogging torque. $\psi_{abc}(i_{abc},\theta)$ is the stator winding flux linkage. $\psi_{rabc}(\theta)$ is the flux linkage contributed by permanent magnets. $L_{abc}(\theta)$ is the inductance matrix of stator winding described as

$$L_{abc}(\theta) = \begin{bmatrix} L_{aa}(\theta) & L_{ab}(\theta) & L_{ac}(\theta) \\ L_{ba}(\theta) & L_{bb}(\theta) & L_{bc}(\theta) \\ L_{ca}(\theta) & L_{cb}(\theta) & L_{cc}(\theta) \end{bmatrix}. \tag{5}$$

As the iron core has the nonlinear magnetization property, the winding inductance is a function of both current and rotor position. For PM machines, their winding magnetic fields are dominated by the permanent magnets, the inductance L_{abc} is considered as rotor position dependent only, expressed as $L_{abc}(\theta)$.

$T_{\text{cog}}(\theta), \psi_{rabc}(\theta)$, and $L_{abc}(\theta)$ profiles are calculated from the nonliner transient FE solution. They are rotor position dependent. In addition, the saturation effect is included in them also.

III. Simulink Implementation

Two types of machine block in Simulink are developed according to (1)–(4). One is referred as the equation based model; the other is referred as the circuit component based model. The equation based model is built by directly writing (1)–(4) using Simulink graphical operation symbols, for example, multiplication, derivative, etc. The circuit component based model is built using circuit components, for example, inductor, VCS, resistor, etc. The equation based model is described as follows; circuit component based model is presented in [4].

Digital Object Identifier 10.1109/TMAG.2005.846122

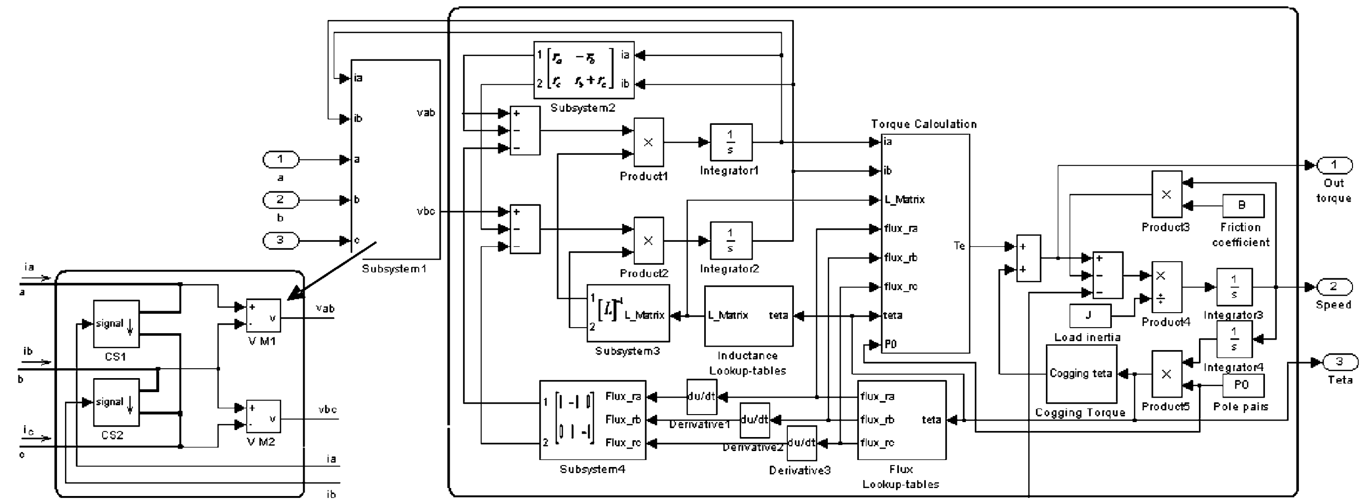

Fig. 1. Equation-based PM motor block.

The voltages applied to the motor are line voltages. For coupling the phase variable model with external circuits, (1) needs to be rewritten with v_{ab} and v_{bc} instead of v_a, v_b, and v_c. For Wye connection winding, one has

$$\begin{bmatrix} v_{ab} \\ v_{bc} \\ v_{ac} \end{bmatrix} = \begin{bmatrix} r_a & -r_b & 0 \\ 0 & r_b & -r_c \\ r_a & 0 & -r_c \end{bmatrix} \begin{bmatrix} i_a \\ i_b \\ i_c \end{bmatrix} + \frac{d}{dt} \begin{bmatrix} \psi_a - \psi_b \\ \psi_b - \psi_c \\ \psi_a - \psi_c \end{bmatrix}. \quad (6)$$

In actual Wye connection winding, the currents i_a, i_b, and i_c satisfy KCL, which enforces the third harmonic components to be zero. Therefore, the following constraint to i_a, i_b, and i_c needs to be considered:

$$i_a + i_b + i_c = 0. \quad (7)$$

Substituting (7) into (6), one can obtain

$$\begin{bmatrix} v_{ab} \\ v_{bc} \end{bmatrix} = \begin{bmatrix} r_a & -r_b \\ r_c & r_b + r_c \end{bmatrix} \begin{bmatrix} i_a \\ i_b \end{bmatrix} + \frac{d}{dt} \begin{bmatrix} \psi_a - \psi_b \\ \psi_b - \psi_c \end{bmatrix}. \quad (8)$$

The state equations are required for performing the simulation in Matlab/Simulink. Substituting (2) into (8) and rearranging it, one can obtain

$$\begin{aligned} \begin{bmatrix} di_a/dt \\ di_b/dt \end{bmatrix} &= \begin{bmatrix} L_{aa} - L_{ab} - L_{ac} + L_{bc} & L_{ab} - L_{bb} + L_{bc} - L_{ac} \\ L_{ba} - L_{ca} - L_{bc} + L_{cc} & L_{bb} - L_{cb} + L_{cc} - L_{bc} \end{bmatrix}^{-1} \\ &\times \left\{ \begin{bmatrix} v_{ab} \\ v_{bc} \end{bmatrix} - \begin{bmatrix} r_a & -r_b \\ r_c & r_b + r_c \end{bmatrix} \begin{bmatrix} i_a \\ i_b \end{bmatrix} \right. \\ &\left. - \begin{bmatrix} 1 & -1 & 0 \\ 0 & 1 & -1 \end{bmatrix} \begin{bmatrix} d\psi_{ra}/dt \\ d\psi_{rb}/dt \\ d\psi_{rc}/dt \end{bmatrix} \right\} \end{aligned} \quad (9)$$

where i_a and i_b are the state variables. Their initial values are set zero. As the value of $\psi_{ri}, (i = a, b, c)$ is retrieved from $\psi_{rabc}(\theta)$ table, using $d\psi_{ri}/dt, (i = 1, b, c)$ directly will cause a very high abnormal pulse at the first simulation step. This phenomenon is avoided by using the following transformation:

$$\frac{d\psi_{ri}}{dt} = \frac{d\psi_{ri}}{d\theta} \cdot \frac{d\theta}{dt} = \frac{d\psi_{ri}}{d\theta} \cdot \omega, \quad (i = a, b, c). \quad (10)$$

Instead of using $d\psi_{ri}/dt, (d\psi_{ri}/d\theta) \cdot \omega$ is used to build the model. As the rotor speed ω equals zero at the first simulation step, the very high pulse can be restrained.

The PM motor block based on state equation (9) and (3)–(4) is shown in Fig. 1.

Three inputs of the block are line voltages; three outputs are the torque, speed, and the rotor position. The resistance matrix, inverse inductance matrix, and the constant matrix of (9) are represented by subsystem 2, 3, and 4, respectively. The rotor position dependence of inductances, flux linkage due to the permanent magnets and the cogging torque are stored in the three lookup-tables. The data retrieving is performed in terms of the rotor position. According to (9), variables i_a and i_b are obtained using integrator 1 and 2. According to (4), angular speed ω is calculated using integrator 3. The rotor position θ is evaluated using integrator 4. Torque calculation block calculates the electromagnetic torque, given by the first two terms on the right-hand side of (3). Adding the electromagnetic torque and the cogging torque, one obtains the total torque.

Up to now, i_a and i_b, v_{ab} and v_{bc} are variables but not circuit signals. In order to connect the equation based model with the external circuit, "subsystem 1" transfers variable i_a and i_b into phase currents, v_{ab} and v_{bc} into line voltages. The phase currents i_a, i_b, and i_c signals are produced through two controlled current sources CS1 and CS2. The Line voltage v_{ab} and v_{bc} are generated by voltage measurement blocks VM1 and VM2.

IV. Various Model Comparison

Comparison is performed on a six-pole surface mounted PM motor.

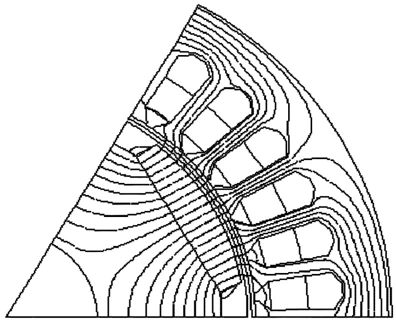

Fig. 2. One pole filed distribution of the 6-pole 36-slot PM motor.

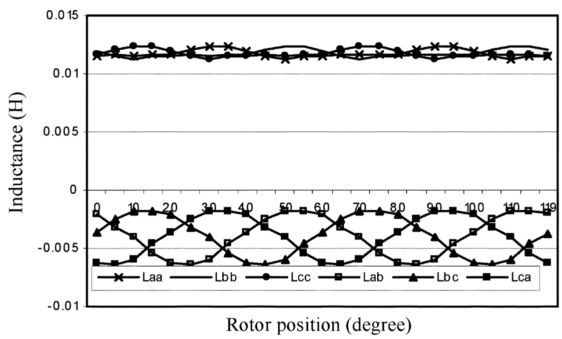

Fig. 3. Rotor position dependence of inductance.

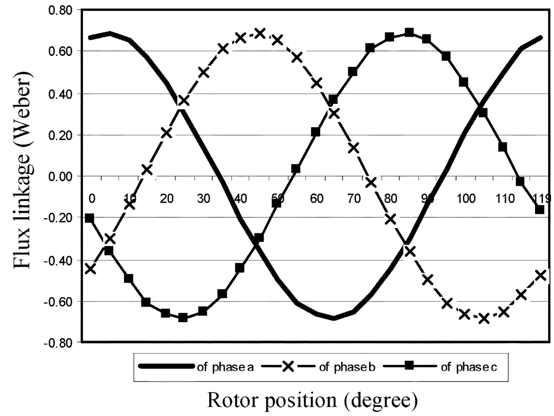

Fig. 4. Rotor position dependence of flux linkage due to PM.

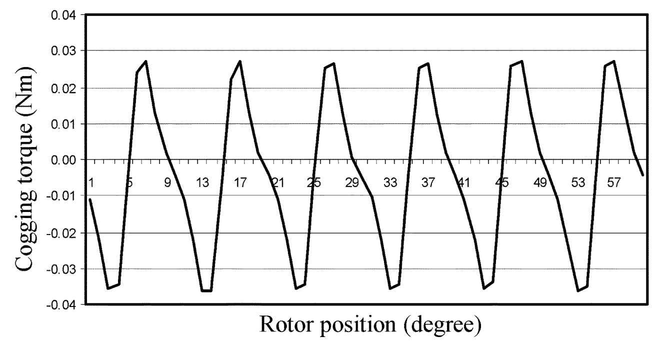

Fig. 5. Cogging torque.

A. Full FE model

A nonliner transient FE model of the PM synchronous is built. The potential equations involving both the electric and magnetic potentials are as follows:

$$-\nabla\cdot\left(\sigma\frac{\partial A}{\partial t}-\sigma v\times(\nabla\times A)+\sigma\nabla V-J^e\right)=0 \quad (11)$$

$$\sigma\frac{\partial A}{\partial t}+\nabla\times(\mu^{-1}\nabla\times A-M)-\sigma v\times(\nabla\times A)+\sigma\nabla V=J^e \quad (12)$$

$$B=\mu_0(H+M). \quad (13)$$

The parameters used in (11)–(13) have their conventional meanings. One pole field solution of the motor being implemented is given in Fig. 2. In addition, using the nonliner transient FE solutions of (11)–(13) with the appropriate boundary conditions, $L_{abc}(\theta), \psi_{rabc}(\theta)$, and $T_{\rm cog}(\theta)$profiles, which is used in the proposed physical phase variable model are obtained, as shown in Figs. 3–5.

B. dq-Model

The dq-model of the PM synchronous motor is also built [3]. The inductances L_d and L_q are obtained by implementing the dq transformation on the dc and fundamental components of inductances profile $L_{abc}(\theta)$. Similarly, the flux linkages ψ_{rd} and ψ_{rq} are obtained by performing the dq transformation on the fundamental components of the flux linkage profile $\psi_{rabc}(\theta)$. Fig. 6 shows the speed control system used for examining the performances of various types of machine models [5]. In order to investigate the intrinsic behavior of the dq-model, the phase variable model and the full FE model, a filtering circuit is added to remove the influences of PWM on torque, voltage, and current profiles.

C. Comparison Results

Fig. 7 gives the torque profiles during the starting process of the PM motor. Before reaching the given speed, the output torque is controlled at the maximum torque 20 Nm.

The output torque equals the required load torque after the motor operates at the given speed. The torque obtained from the phase variable model is very close to the one from the full FE model. Under this excitation condition, the dq-model gives a very smooth torque as it ignores the harmonic effects caused by the pole shape, rotor position dependence of inductance, flux linkage, as well as the cogging torque.

V. Application Example

A commonly-used PWM vector control speed regulation system is built in Simulink. Fig. 8 shows the simulation results obtained using the proposed phase variable model. The fluctuations in the back electromotive force (EMF) waveform, Fig. 8(a), show the effects of the permanent magnet pole shape as well as the rotor iron surface. These effects are contained in the waveform of flux linkage contributed by the permanent magnets, shown in Fig. 4. The harmonic components existing in the voltage profile, shown in Fig. 8(b), are from back EMF, rotor position dependent inductance shown in Fig. 3, the PWM excitation pattern, as well as the current. The pulsations of the torque profile in Fig. 8(c) are composed of cogging torque and ripple torque components. The cogging torque, shown in Fig. 5,

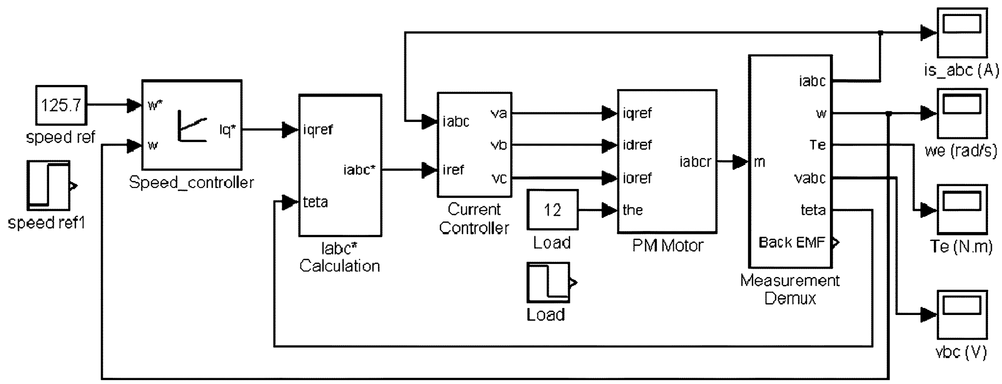

Fig. 6. Integrated drive system.

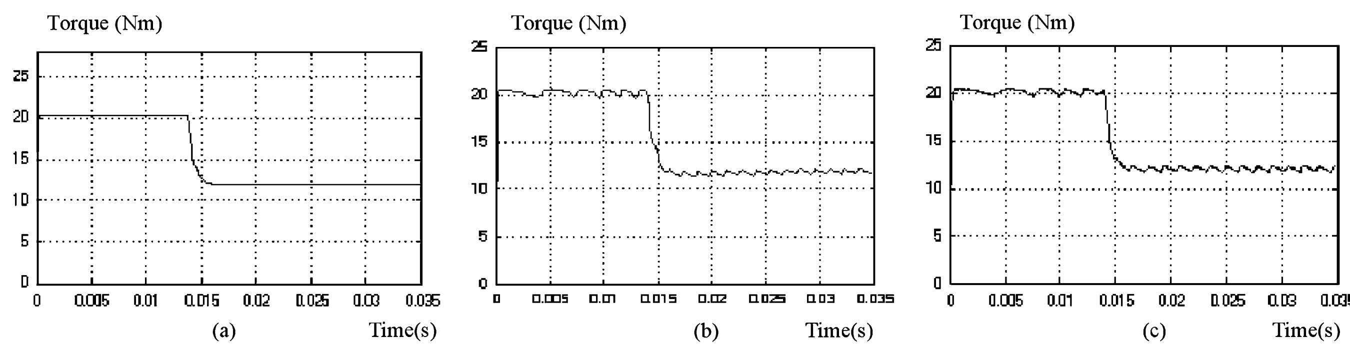

Fig. 7. Torque profile obtained by (a) dq-model, (b) FE model, and (c) physical phase variable model.

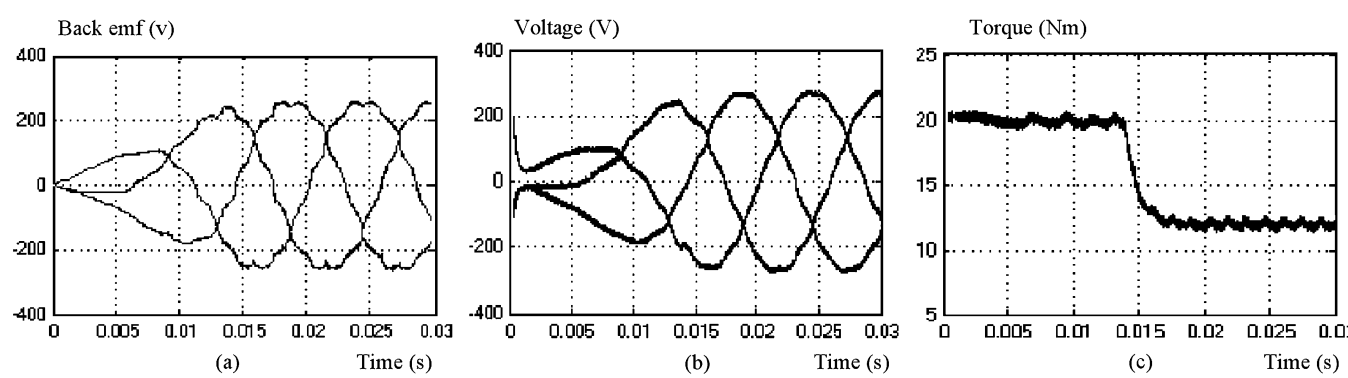

Fig. 8. (a) Back EMF. (b) Voltage. (c) Torque profile obtained by using a physical phase variable model in a PWM drive system.

arises from the variation of the magnetic permeance of the stator teeth and slots. The ripple torque occurs as result of fluctuations of the working flux distribution and the armature MMF. All these effects are ignored in the dq-model.

VI. Conclusion

A physical phase variable model of PM machines for the purpose of integrated drive system simulations is developed and verified. The developed model uses transient FE solutions to establish a detailed block description of the implemented machines in Simulink. The established model provides the same performance in application as the full utilization of FE models but with much faster simulation speed.

The proposed model can be used for the evaluation of various machine designs as well as plug and play machine drives components and their practical control strategies.

Acknowledgment

This work was supported in part by a grant from the Office of Naval Research.

References

[1] V. Petroviæ and A. M. Stankoviæ, "Modeling of PM synchronous motors for control and estimation tasks," in *Proc. 40th IEEE Conf. Decision and Control*, Dec. 2001, pp. 2229–2234.
[2] A. B. Proca, A. Keyhani, and A. EL-Antably, "Analytical model for permanent magnet motors with surface mounted magnets," *IEEE Trans. Energy Convers.*, vol. 18, no. 3, pp. 386–391, Sep. 2003.
[3] A. E. Fitzgerald, C. Kingsley, and S. D. Umans, *Electric Machinery*, 6th ed. New York: McGraw-Hill, 1990, pp. 248–252.
[4] O. A. Mohammed, S. Liu, and Z. Liu, "A phase variable model of brushless dc motors based on finite element analysis and its coupling with external circuits," *IEEE Trans. Magn.*, vol. 41, no. 5, pp. 1576–1579, May 2005.
[5] B. K. Bose, *Modern Power Electronics and ac Drives*. Englewood Cliffs, NJ: Prentice-Hall, 2001, pp. 381–387.

Manuscript received June 8, 2004.